UC Irvine
UC Irvine Previously Published Works

Title
Signatures of Through-Space Charge Transfer in Two-Photon Absorption of Paracyclophane Derivatives

Permalink
https://escholarship.org/uc/item/0s29g5h1

Journal
Bulletin of the Korean Chemical Society, 40(11)

ISSN
1225-0058

Authors
Salimi, Abbas
Cho, Daeheum
Lee, Jin Yong
et al.

Publication Date
2019-11-01

DOI
10.1002/bkcs.11874

Peer reviewed

Signatures of Through-Space Charge Transfer in Two-Photon Absorption of Paracyclophane Derivatives

Abbas Salimi,[†,‡] **Daeheum Cho,**[†,*] **Jin Yong Lee,**[†,*] **Sunwoo Kang,**[§,*] **and Shaul Mukamel**[¶,*]

[†]*Department of Chemistry, Sungkyunkwan University, Suwon 16419, South Korea.*
*E-mail: daeheumc@uci.edu; jinylee@skku.edu
[‡]*School of Chemical Engineering, Sungkyunkwan University, Suwon 16419, South Korea*
[§]*Display Research Center, Samsung Display Co., 1 Samsung-ro, Giheung-gu, Yongin, Gyeonggi, South Korea. *E-mail: swkang821221@gmail.com*
[¶]*Department of Chemistry, University of California, Irvine, CA, 92697, USA.*
*E-mail: smukamel@uci.edu

Third order polarizability, (γ) taken from the collective electronic oscillator (CEO) method was used to calculate the two-photon absorption (TPA) of tetrastyryl-[2,2]paracyclophane derivatives with different through-space charge transfer configurations considering various donor and acceptor combinations at the terminal styryl groups. For the virtually same linear absorption, different TPA spectra were obtained. For controlling and fine-tuning frequency and cross-sections of TPA the through-space charge transfer interactions can be used. The results are explained by the electronic density matrices corresponding to governing oscillators in one- and two-photon absorption and the ground state. It is indicated that for the studied systems mainly the lowest four oscillators are responsible for the TPA cross-sections rather than a simple effective three-state model.

Keywords: Two-photon absorption, Paracyclophanes, Collective electronic oscillator, Through-space charge transfer

Introduction

Two-photon absorption (TPA) as a nonlinear absorption process where a pair of photons is absorbed simultaneously attracted a lot of attention due to fast improvements in experiments and new applications.[1,2] Organic molecules that have large TPA cross-sections can be applied in, 3D optical data storage, fluorescence microscopy,[3] and amyloid beta plaques imaging.[4]

These applications stem primarily from the ability to access high-energy excited states by low-energy laser sources. The quadratic dependence of simultaneous absorption rate of two photons on the laser intensity is the origin of 3D spatial resolution.

Using tightly focused beam leads to highest intensity at the focus and decreases as z^{-2} where is z is the distance from the focal plane, when distances are longer than the Rayleigh length. Thus, the TPA rate decreases very rapidly as z^{-4} and the excitation is narrowed in a small volume around the focus. This should facilitate imaging applications in absorbing or scattering media, such as biological tissues.[5] Many applications require chromophores with a large TPA cross-section because a stronger response can be induced by lower laser powers. Understanding the relationship between the TPA cross-section and the molecular structure could help provide guidelines for synthetic strategies for novel TPA

chromophores and could suggest further applications. An increased TPA cross-section has been obtained by extending π-conjugation length and the introduction of electron donor (D) and acceptor (A) groups at the ends of chain and in every part of the conjugation sequence. For push-pull molecules, disubstituted by both donor and acceptor groups, a strong TPA resonance was reported because of intramolecular charge transfer (ICT).[6,7] This is due to the large transition dipole moment and the difference of dipole moment between the ground and the ICT excited states. A three-state approximation could not reproduce the ICT TPA spectrum of dialkylaminonitrostilbene.[8,9] The TPA spectrum of 4-(diethylamino)-β-nitrostyrene (DEANST) has been measured in solution and in crystals.[10] In solution, the TPA spectra can be explained by the relevant one-photon absorption spectrum related to the ICT. On the contrary, the one- and two-photon resonances in crystals have been found to correspond to different electronic transitions.

A new design strategy has been suggested based on the cooperative enhancement of TPA in multi-branched structures,[11] that two and three two-photon active asymmetric donor–acceptor chromophores connected using an amine group. The trimer TPA cross-section compare to the monomer was more than six times larger instead of additive three times. Delocalization effect alone cannot explain this enhancement,[12] and it was suggested that charge redistribution may influence

the dipole terms. A systematic theoretical framework is needed to explain this cooperative enhancement. Macak et al.[13] performed *ab initio* calculations to investigate the TPA cross-section increasing as a function of the number of branches, and a significant vibronic contribution to the cross-section was observed.

It has been argued that the symmetrically substituted D–π–D conjugated molecules give rise to a large TPA cross-section. This enhancement has been connected to intramolecular charge transfer between the terminal donor groups to the central π-bridge.[14–16] These molecular systems are linear quadrupolar molecules with surprisingly large TPA cross-sections. An *ab initio* study of the molecular family (A–π–A and D–π–D) revealed that as the donor-acceptor coupling strength enhances, the product of the transition dipole moments increases and the energy differences appearing in the expression for the TPA cross-section decrease.[17] Furthermore, the cross-section and the off-resonant first hyperpolarizability, β (0), have a good linear relationship.[18] Ratner et al. have proposed a different strategy to increase the TPA cross-section in molecular chromophores.[19] They investigated the relationship between molecular conformation and the TPA properties in a class of alkyl-substituted 4-quinopyran, and maximized the TPA cross-section by twisting the molecule around the bond that connects the chromophore donor and acceptor phenylene sequences. Drobizhev et al. reported a record high TPA cross-section measured with femtosecond pulses in a dendrimer comprised of 29 repeat units of 4,4′-bis(diphenylamino)stilbene chromophore.[20] They concluded that it is possible to obtain large TPA cross-section in higher generations.

Some methods have been used to obtain the nonlinear optical susceptibilities. Among them Ward's pertubative sum-over-state (SOS) method is a popular approach.[21–26] It can be applied successfully for the experimentally determined magnitudes. A quantitative analysis has been applied for aromatic molecules to describe the multiply excited configurations to find the states with the significant contribution to the SOS expansion.[27,28] Different methods have been suggested to find the these dominant state and their connection with certain molecular features. Especially, when the charge transfer is critical the two-state model is suitable for quadratic optical polarizabilities description.[29–32] To assess the static hyperpolarizabilities of charge transfer the finite-field method would be the another option,[33–35] which is commonly used in quantum chemistry softwares. Compare to SOS method, the finite-field mainly focuses on wavefunctions of ground-state. Thus it is not possible to indicate the dominant excited states of nonlinear optical properties using that.

The CEO formalism[36–43] provides a more general approach that can be used for both off resonant and resonant responses. To obtain the off-resonant hyperpolarizabilities of push-pull carotenoids the CEO framework was applied.[44] It was used for frequency-dependent resonant optical properties as well.[45] (4-(4-dihexylaminostyryl)-16-(4-nitrostyryl)[2,2]paracyclophanes) with through-space charge transfer have been synthesized.[46] Absorption spectra and the off-resonant first
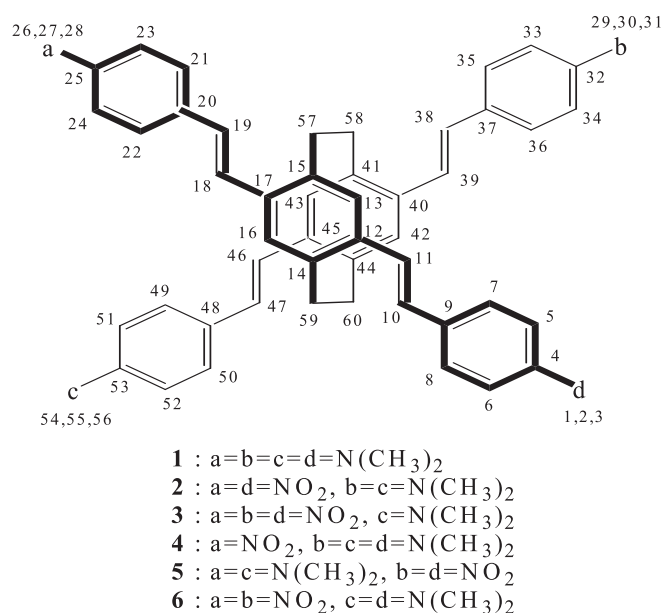

1 : a=b=c=d=N(CH₃)₂
2 : a=d=NO₂, b=c=N(CH₃)₂
3 : a=b=d=NO₂, c=N(CH₃)₂
4 : a=NO₂, b=c=d=N(CH₃)₂
5 : a=c=N(CH₃)₂, b=d=NO₂
6 : a=b=NO₂, c=d=N(CH₃)₂

Figure 1. Tetrastyryl-[2,2]paracyclophane derivatives and their atomic numbering.

hyperpolarizabilities were carried out using the CEO method[47] considering different through-space charge transfer network.

In this paper we investigate one- and two-photon absorption of these molecules. The tetrastyryl-[2,2]paracyclophane has derivatives with donor or acceptor group at the four terminal styryl groups. Depending on the combination of donors and acceptors, both through-space and through-bond charge transfer or only through-space charge transfer can take place. The various tetrastyryl-[2,2]paracyclophane molecules
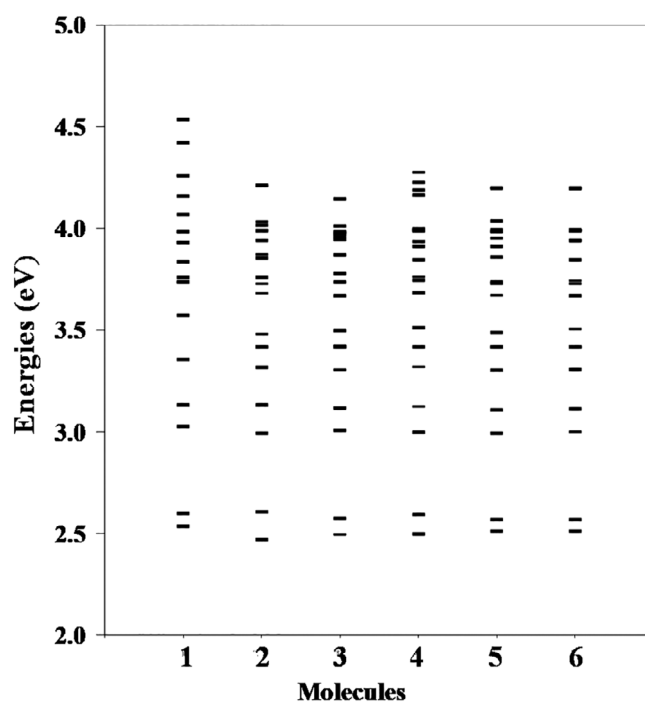

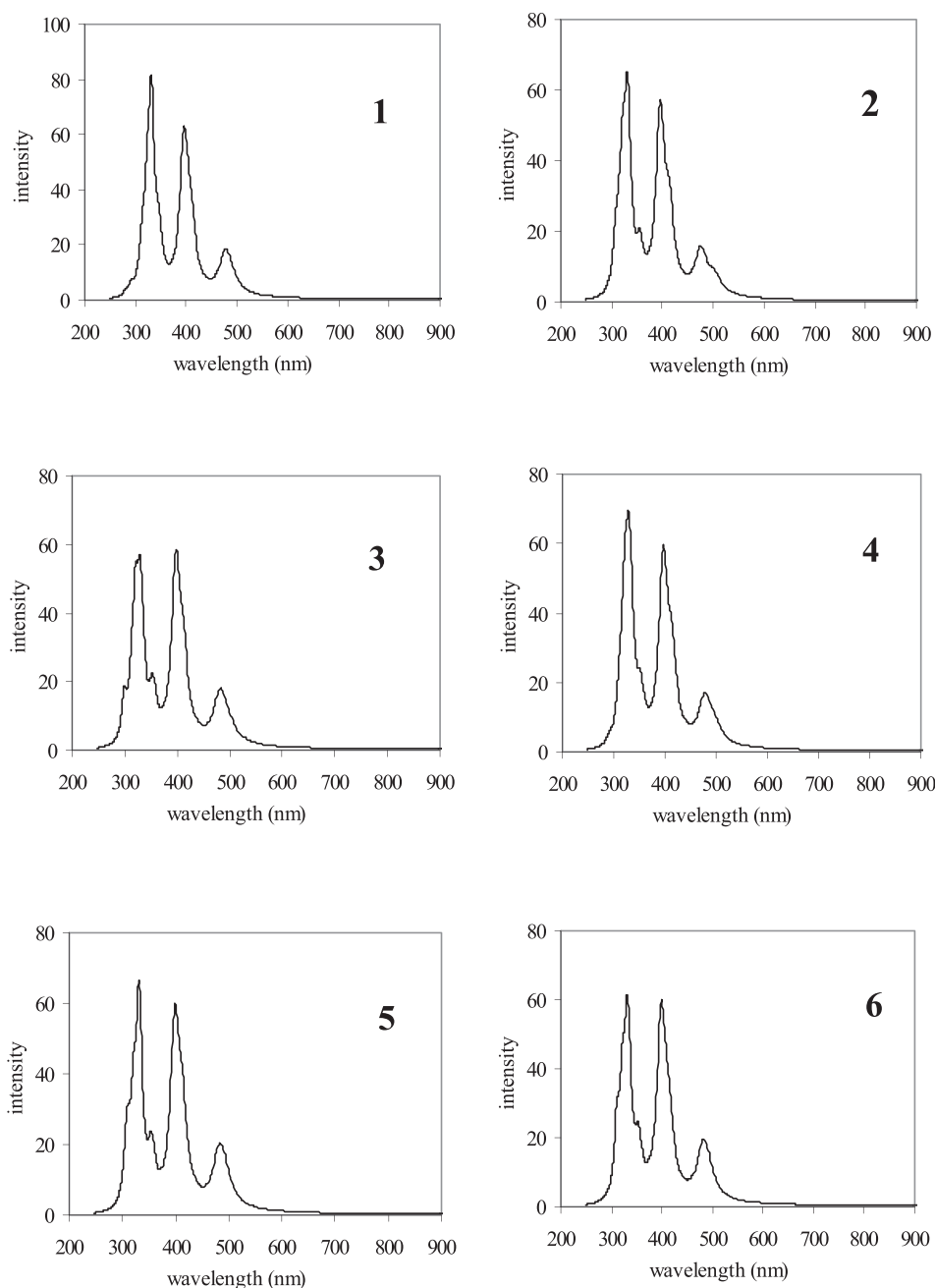**Figure 2.** Energies of the 20 lowest excited states of **1–6**.

Figure 3. Linear absorption spectra [Im($\alpha(\omega)$) in 10^{-23} esu] of tetrastyryl-[2,2]Para-cyclophane derivatives.

obtained by combination of electron donor and acceptor are shown in Figure 1.

Presenting the electronic oscillators in the atomic basis set provides a very intuitive picture of the molecule behavior during the course of the TPA process.

Linear Absorption

The INDO/S semiempirical Hamiltonian which was constructed to reproduce the spectra of simple molecules at the singly excited CI level was used. This Hamiltonian provided by Pople[48,49] and parameterized by Zerner *et al.*[50–53]

is often applied in optical response computations. INDO/CIS computations have been used to study the excited states of various chromophores including transition metals[50,51,53] and transition density which shows good agreement with experiments for monomeric state.[54]

The combination of time-dependent Hartree–Fock (TDHF)[56] and the INDO/S Hamiltonian without further parameterization for most molecules is applicable and thus gives an alternative way for calculating the optical properties of a broad range of molecules.[45] At first semiempirical AM1 methods was employed for geometry optimization.[55] TDHF equations of motion for the density matrix in Liouville space

Table 1. Linear absorption wavelength (λ_{LAi}) and two-photon absorption wavelengths (λ_{TPAi}) and intensities ($\sigma_{2,TPAi}$) for tetrastyryl-[2,2]paracyclophanes.[a]

	1	2	3	4	5	6
λ_{LA1}	478	477	482	478	484	482
λ_{LA2}	397	396	398	397	400	400
λ_{LA3}	330	330	329	329	331	331
λ_{TPA1}	596	712	673	704	673	673
$\sigma_{2,TPA1}$[b]	47.1	10.3	17.6	4.4	15.9	13.4
$\sigma_{2,TPA1}$[c]	72.2	20.1	29.3	9.5	27.4	24.1
λ_{TPA2}	548	677	620	673	616	645
$\sigma_{2,TPA2}$[b]	20.6	4.8	6.2	5.1	6.4	10.1
$\sigma_{2,TPA1}$[c]	31.8	11.2	11.9	11.6	11.8	16.7
λ_{TPA3}		590		587		
$\sigma_{2,TPA3}$[b]		25.5		34.9		
$\sigma_{2,TPA3}$[c]		45.0		58.4		

[a] The wavelengths are in nm and the intensities in 10^{-34} esu.
[b] These values are obtained from only diagonal terms of second hyperpolarizabilities, $Im(\gamma_{xxxx} + \gamma_{yyyy} + \gamma_{zzzz})/5$.
[c] These represent orientationally averaged values as described in the text.

was then solved to get the frequency-dependent nonlinear responses. Solving the TDHF equations includes the diagonalization of the Liouville operator which is effectively done by Krylov-space techniques such as iterative density matrix spectral moment analysis (IDSMA),[57,58] Lanczos,[59] and Davidson's[60,61] algorithms. In the present simulations we used the Lanczos algorithm. The resulting density matrices have clear physical interpretation. After the transformation from the orbital to the atomic basis, the diagonal elements ($n = m$) of the density matrix the charge at mth atom is shown by (ρ_{nm}), while the off-diagonal elements ($n \neq m$) represent the coherence. The off-diagonal elements of the ground-state density matrix reflect the chemical bonding between nth and mth atoms. For the time-dependent density matrix ($\rho(t) = \overline{\rho} + \delta\rho(t)$), the matrix elements $\delta\rho_{nm}(t)$ show the changes in the density matrix induced by an external electric field. $\delta\rho_{nn}(t)$ represents the net charge induced on the nth atom, while $\delta\rho_{nm}(t)$ ($n \neq m$) is a dynamical bond order representing the joint amplitude of finding an electron on mth atom and a hole on nth atom. The CEO code calculates transition densities $(\xi_{nm})_{\nu} = \langle \nu | c_m^{\dagger} c_n | g \rangle$ associated with transition between ground state $|g\rangle$ and excited state $|\nu\rangle$ and relevant transition energies Ω_{ν} which are further applied to compute the oscillator strengths, linear absorption, transition dipoles, and frequency-dependent nonlinear responses.

The electronic oscillator picture has conceptual and numerical benefits comparing to the eigenstate picture (SOS). Instead of taking into account a basis set of eigenstates of the Hamiltonian to represent the wavefunction, a basis of oscillators to show the reduced one electron density matrix was used. Two-dimensional plots of the resulting transition density matrices allow the

analysis of each electronic transition and molecular optical responses concerning electrons and holes excited state charge distribution and motions of in real space. The linear absorption and TPA cross-sections given by the imaginary part of polarizability [$Im(\alpha(\omega))$] and second hyper-polarizabilities [$Im(\gamma(-\omega;\omega,-\omega,\omega))$] were computed using the closed expressions given in Ref.45.

Figure 2 shows the energy eigenstates obtained by the CEO algorithm using the lowest 20 oscillators. As is often the case, the energies of molecules with electron donating group (*e.g.* molecule **1**) are higher than those with electron withdrawing groups (*e.g.* molecule **3**), as presented in Figure 2. The linear absorption spectra ($Im(\alpha_{xx} + \alpha_{yy} + \alpha_{zz})$) with line width of 0.08 eV are shown in Figure 3 and the corresponding resonance frequencies are given in Table 1. The linear absorption spectra are very similar in all molecules. They show three peaks (LA1, LA2, and LA3 starting from the low energy). The LA1 show a bit larger variation among molecules (about less than 4 nm) than other peaks. Molecules **3**, **5**, and **6** have red-shifted frequencies by about 5 nm compared to **1**, **2**, and **4**, while other absorption peaks do not change at all. The peaks around 330 nm (LA3) only show a little variation around 1 nm. The lowest two oscillators are responsible for the first linear absorption peak (LA1), and the next two oscillators give the second linear absorption peak (LA2).

The contour maps of the density matrices for the ground-state and the transition density matrices for the dominating oscillators LA1, LA2, and LA3 are depicted in Figure 4. The density matrices for the ground state are virtually the same. The contour map is better understood from the scheme showing blocks in which coherences (off-diagonal parts) and charges (diagonal parts) are represented by bold lines in each block. To represent the electron–hole coherences, the abscissa and ordinate represent the electron and hole axes, respectively.

Hence, the density matrices are not symmetric along the diagonal. However, we only show the upper triangular blocks in the scheme. The four electron donating groups result in the electrons localization and a strong coherence between the two central cyclophane rings by through-space interactions for LA1 peaks. Third and fourth oscillators, compared with the first and the second modes, have electrons with more diffusion on the styryl groups at the 397 nm. The coherence between central cyclophane rings and the terminal styryl groups is observable for the 330 nm peak.[62]

Two Photon Absorption

The CEO method has reproduced the experimental absorption spectra very consistently as described in the introduction section.[47,63,64] To validate the CEO method for the study of TPA spectra, we compared the TPA properties obtained by CEO method for bis-donor-substituted π-conjugated molecules A, B, and C (Scheme 1) with previous experimental and theoretical results.[14,15] In the
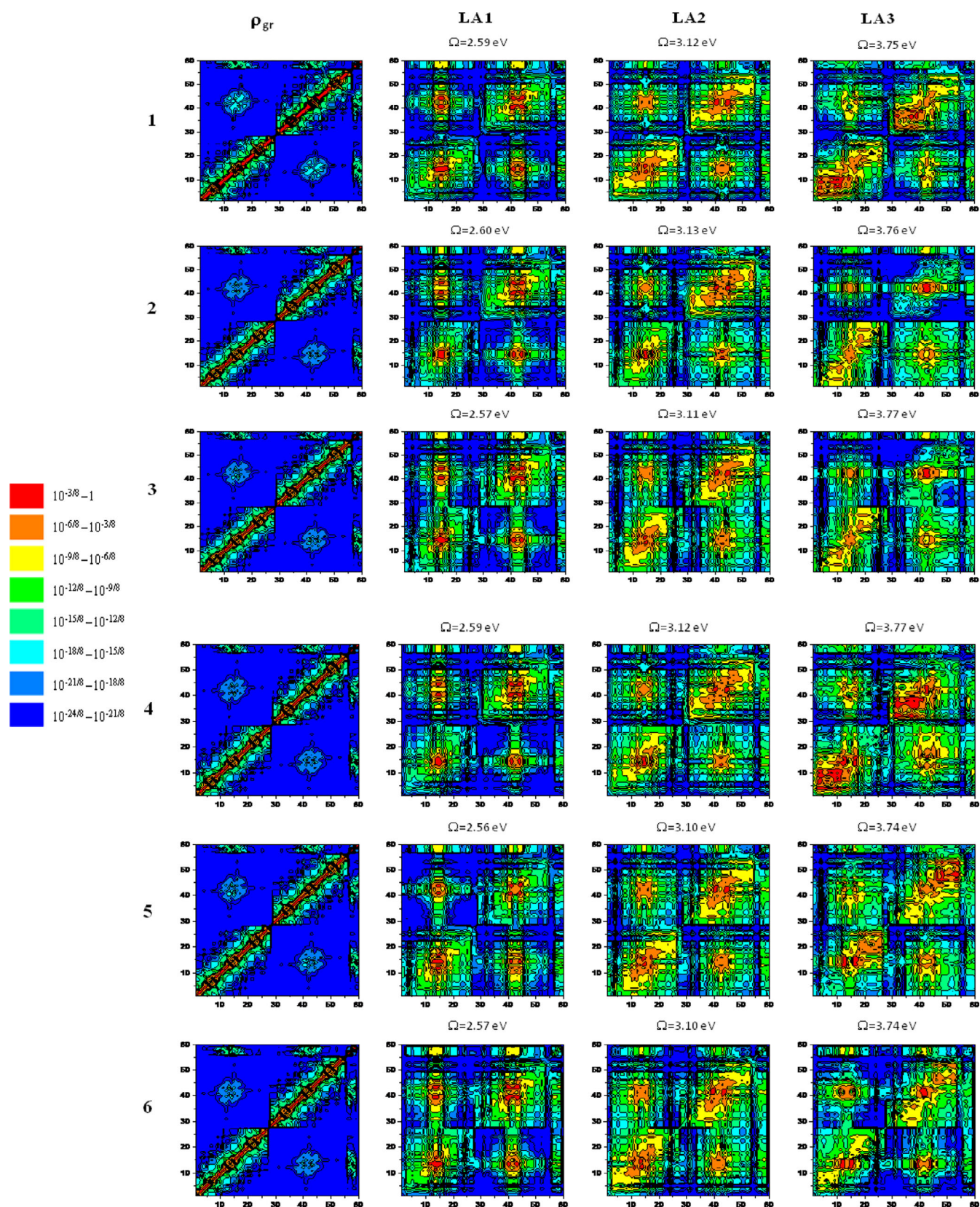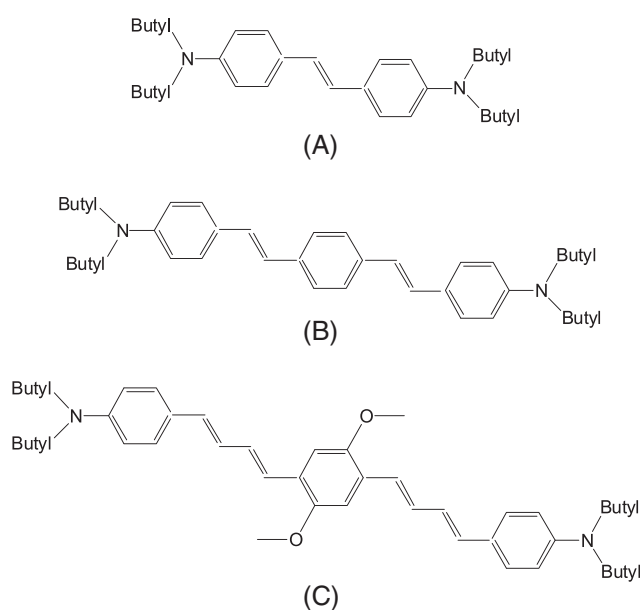
Figure 4. Contour plots of ground-state density matrices (ρ_{gr}) and the oscillators which are most dominant for three linear absorption peaks (LA1, LA2, and LA3) of tetrastyryl-[2,2]paracyclophane derivatives. The legend gives a fraction of maximum values for ρ_{gr}, LA1, LA2, and LA3.

Scheme 1. Bis-donor-substituted π-conjugated molecules.

calculations, the butyl groups are replaced by methyl groups as done in the previous calculations.[15] The peak intensities and frequencies are given in Table 1. The intense peaks around 400 nm originate from linear absorption states not from TPA states. In particular, the TPA spectra below 500 nm are not properly described from the current CEO calculations because much more oscillators should be included to describe accurately those TPA states, which is impractical for large molecules. In contrast to the linear absorption, the TPA spectral features are quite different. The resonance frequencies and the intensities of TPA are listed in Table 1. Table 2 lists the TPA wavelengths ($\lambda^{(2)}_{max}$) and their relative TPA intensities for **A**, **B**, and **C**. The experimental $\lambda^{(2)}_{max}$ values were reported to be 605, 730, and 775 nm for **A**, **B**, and **C**, respectively. Our CEO calculations give that those are 504, 539, and 574 nm, which are consistent and comparable with the previously calculated values of 529, 595, and 620 nm. In theoretical calculations, the TPA wavelengths were blue-shifted compared with the experimental results, however, the trend is consistent. On the other hand, the relative TPA intensities are in good

agreement with experimental and theoretical results. Thus, the CEO method could be an efficient way to study the TPA spectra of complicated organic compounds. To calculate TPA the lowest 20 modes have been used. The TPA cross-section is proportional to the imaginary part of the frequency-dependent second hyperpolarizability.

$$\sigma_{TPA}(\omega) \sim \omega^2 \mathrm{Im}\gamma(-\omega;\omega,-\omega,\omega) \tag{1}$$

Figure 5 shows σ computed using only diagonal tensor elements $(\mathrm{Im}(\gamma_{xxxx} + \gamma_{yyyy} + \gamma_{zzzz})/5)$ orientationally averaged[19] with 0.08 eV line width. The relevant TPA spectra are represented as insets in the Figure 5 with units in 10^{-34} esu. The TPA can locate approximately 0.3–0.9 eV higher than the first and the second linear absorption peaks like the linear quadrupolar systems of bis-donor diphenylpolyene and bis-styrylbenzene derivatives,[62] while as opposed to linear polyenes and some of α,ω-substituted polyenes that the possible one-photon state locates at somewhat higher energy state.[65,66]

To pinpoint the contribution of off-diagonal terms we investigated the orientationally averaged γ in the photon energy range of 1.6–2.6 eV which covers all the TPA peaks. These γ values are obtained by[23]:

$$\gamma = \left[3\sum_{i}\gamma_{iiii} + \sum_{i\neq j}\left(2\gamma_{iijj} + \gamma_{ijji}\right)\right]/15 \tag{2}$$

here i and j run over the x, y, and z components. The resulting TPA spectra are shown in Figure 6. The graphs are almost identical to the insets of Figure 5. The corresponding peak intensities and frequencies are listed in Table 3. As may be seen from Table 3, the contributions of off-diagonal terms are significant in all the molecular systems. Figure 7 shows the contour maps of the transition density matrices for the modes relating to the TPA1 and TPA2 states. A large coherence length for all molecules, especially between the central cyclophane ring and the counter molecular parts can be seen. In addition to the oscillators corresponding to TPA1 and TPA2, we have investigated all other modes, and found that they have a very short coherence length, *i.e.*, the density matrices are

Table 2. Calculated relative two-photon absorption intensities (I_{rel}) and peak positions ($\lambda^{(2)}_{max}$ in nm) for A, B, and C for the theoretical results, A′, B′, and C′ are model compounds for A, B, and C, wherein butyl groups on amino moieties were replaced by methyl groups.

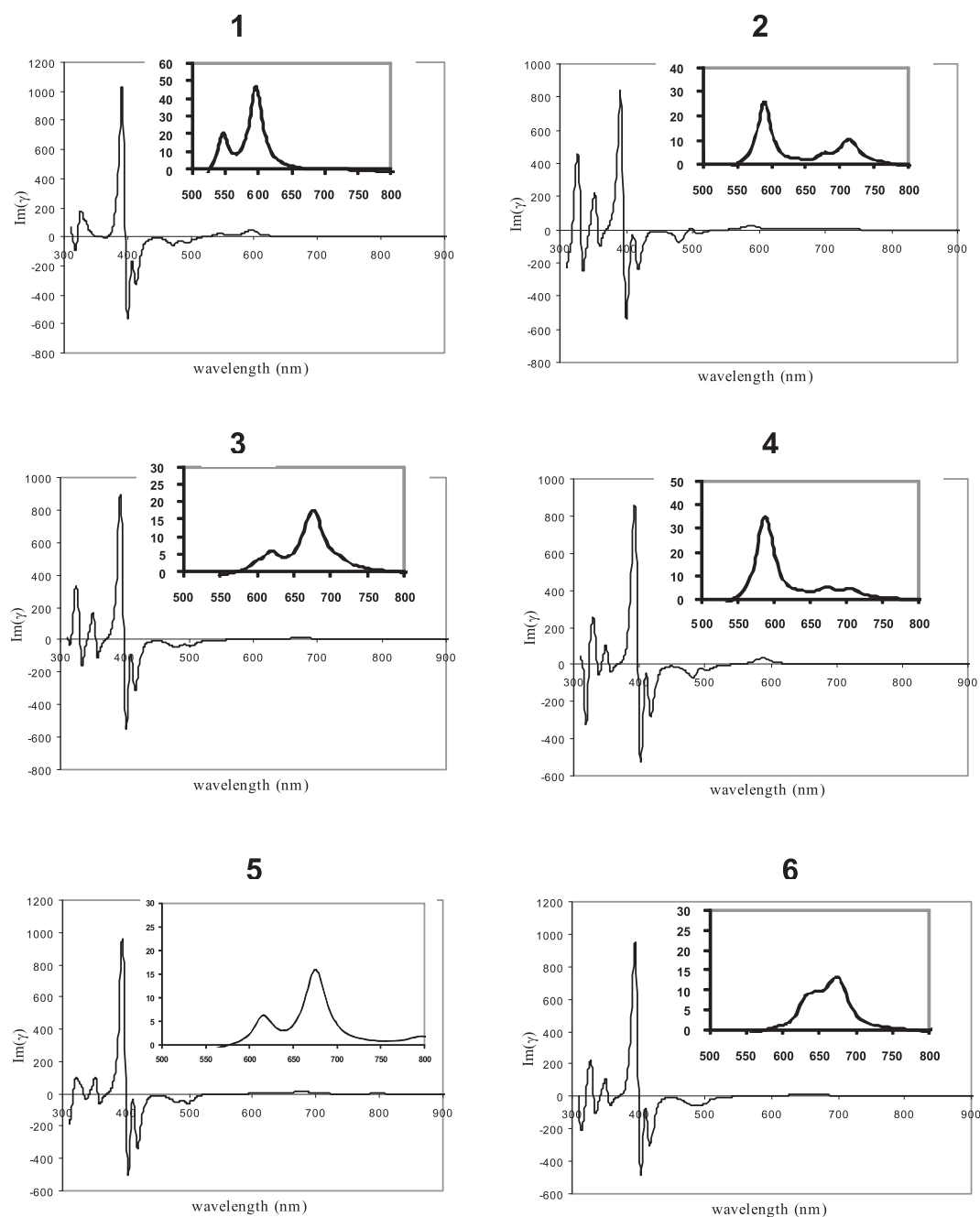|	This work				Previous work		
	Theoretical		Theoretical14		Experimental14		
Compound	$\lambda^{(2)}_{max}$	I_{rel}	$\lambda^{(2)}_{max}$	I_{rel}	Compound	$\lambda^{(2)}_{max}$	I_{rel}
A′	504	1.0	529	1.0	A	605	1.0
B′	539	3.1	595	3.4	B	730	4.7
C′	574	3.9	620	3.5	C	775	6.0

Figure 5. Two-photon absorption spectra [Im(γ ($-\omega$; $\omega, -\omega$, ω)) in 10^{-34} esu] using only diagonal elements of tetrastyryl-[2,2]para-cyclophane derivatives. To show the behavior of the second hyperpolarizability only, the ω^2 term of Eq. (1) is not considered. 1 esu is 4.11×10^{-18} cm$^4 \cdot$s/photon.

nearly diagonal. For molecule **2**, the coherence is just in lower triangular region of the contour map so it can be observed only in one direction.

It may happen because in molecule **2** to make a cyclophane two donors in upper para-distyrylbenzene and two acceptors in lower one connected by two ethylene linkers. Electron transfer in here is unidirectional, through-space, from the donor-substituted distyrylbenzene to the acceptor-substituted one for TPA1, while

direction for TPA2 is opposite. However, in other molecular systems except **1** where all the substitutes are donors, the electron transfers both through space and through bond within one of the para-distyrylbenzens. To better understand the properties of these systems, we computed the TPA cross-sections including only contributions from oscillators which lie lower than the TPA state using the three state approximation and compared with the CEO which included dipolar contribution
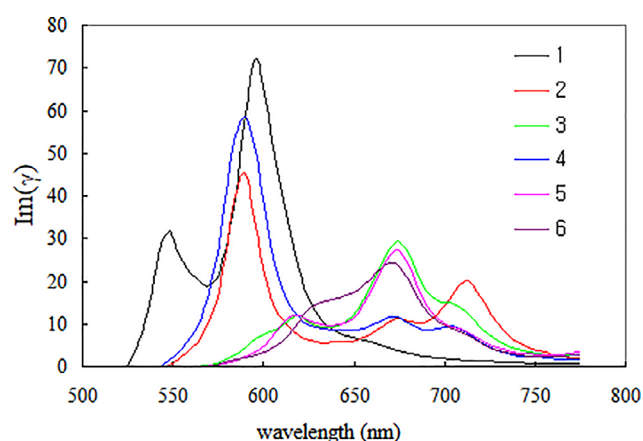
Figure 6. Orientationally averaged TPA spectra (in 10^{-34} esu) of **1–6**.

arising from all the states as well as anharmonicities. The three state expression for the TPA resonance for the $S_O \rightarrow S_f$ transition is

Table 3. Transition dipole moments (μ_{i-j} in eÅ) and energies (Ω in eV) of corresponding states corresponding.

|	1	2	3	4	5	6
μ_{0-1}	0.47	0.53	0.48	0.50	0.55	0.45
μ_{0-2}	0.90	0.86	0.91	0.88	0.93	0.95
μ_{0-3}	1.08	1.08	1.05	1.13	1.09	1.09
μ_{0-4}	1.78	1.72	1.72	1.74	1.74	1.73
μ_{1-TPA1}	0.77	1.35	0.64	0.93	0.48	0.31
μ_{2-TPA1}	1.06	0.36	0.79	0.32	0.75	0.83
μ_{3-TPA1}	0.64	0.95	0.70	0.67	0.69	0.58
μ_{4-TPA1}	0.99	0.47	0.89	0.37	0.85	0.74
μ_{1-TPA2}	0.02	0.70	0.67	0.65	0.81	0.12
μ_{2-TPA2}	0.38	0.36	0.84	0.39	0.58	0.66
μ_{3-TPA2}	0.06	0.63	0.26	0.62	0.15	0.30
μ_{4-TPA2}	0.62	0.28	0.39	0.34	0.19	0.59
Ω_1	2.53	2.47	2.49	2.49	2.51	2.51
Ω_2	2.60	2.61	2.57	2.59	2.57	2.57
Ω_3	3.03	2.99	3.01	3.00	2.99	3.00
Ω_4	3.13	3.13	3.12	3.12	3.10	3.11
Ω_{TPA1}	4.16	3.48	3.67	3.51	3.67	3.67
Ω_{TPA2}	4.54	3.68	4.01	3.68	4.03	3.85
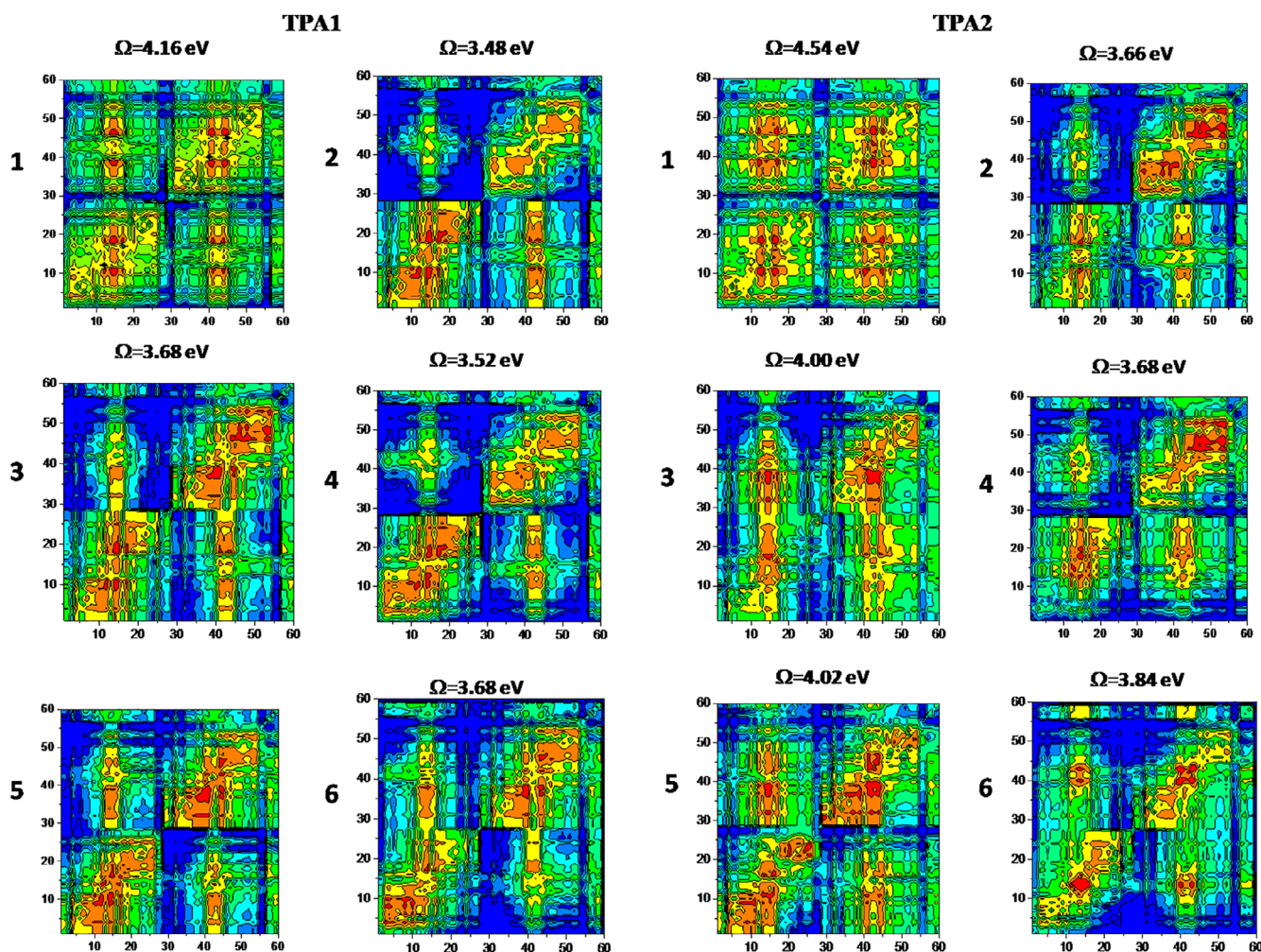
Figure 7. Contour plots of oscillators which are responsible for two TPA peaks (TPA1 and TPA2) of tetrastyryl-[2,2]paracyclophane derivatives. See Figure 4 for legends.
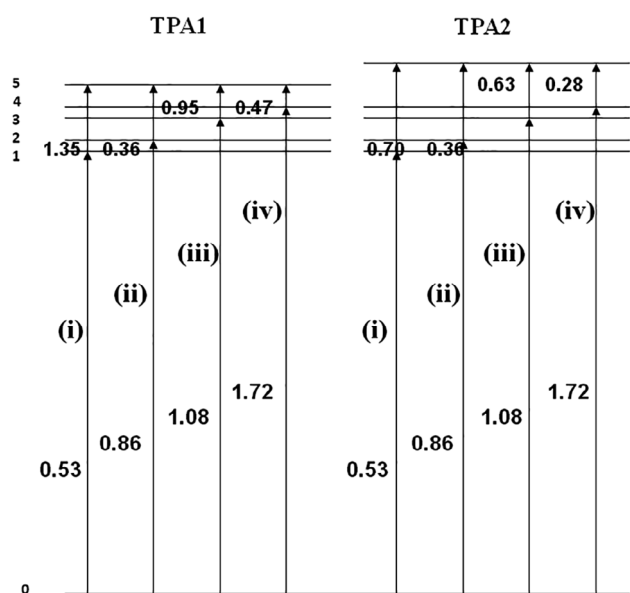
Figure 8. Schematic representation of transition dipole moments of **2**. The optical transition energies correspond to 2.49, 2.57, 3.01, and 3.12 eV, while those of TPA1 and TPA2 states are 3.67 and 4.01 eV, respectively. Vertical arrows represent the electronic transitions, $|0> \to |1> \to |5>$, $|0> \to |2> \to |5>$, $|0> \to |3> \to |5>$, and $|0> \to |4> \to |5>$ for TPA1 and TPA2.

$$\delta(\omega) = \sum_i \frac{M_{0i}^2 M_{if}^2}{(E_i - E_0 - \hbar\omega)^2 \Gamma} \quad (3)$$

where *0*, *i*, and *f* refer to the ground, intermediate, and TPA resonance states, respectively. Γ, E_i, and M_{ij} are the dephasing rate (0.08 eV), energy of state *i*, and the transition dipoles from *i* to *j* state, respectively, and $\hbar\omega = (E_f - E_0)/2$. Table 3 lists the transition dipole moments and optical transition energies. In CEO, the transition dipole moments are approximated by

$$\mu_{\alpha\beta} Tr\left([\bar{\rho}, \xi_\alpha][\mu, \xi_\beta]\right) = Tr\left(\mu(I - 2\bar{\rho})(\xi_\alpha\xi_\beta + \xi_\beta\xi_\alpha)\right)$$

where μ, $\bar{\rho}$, and ξ_α are dipole, ground-state density and interband parts of the time-dependent single electron density matrix, respectively, and the *I* is the identity matrix.[45] The more accurate expression for the transition dipoles is available in our previous study.[67] The electron–hole part of the density matrix can be expanded as

$$\xi(t) = \sum_{\alpha > 0}\left[\xi_\alpha z_\alpha(t) + \xi_\alpha^\dagger z_\alpha^*(t)\right]. \quad (4)$$

The oscillator amplitudes come in complex conjugate pairs z_α and z_α^*, and satisfy the relations $\xi_{-\alpha} = \xi_\alpha^\dagger$. Here, ξ_α is an oscillator represented using the two operator ξ_α and $\xi_\alpha^\dagger$. Figure 8 shows a schematic diagram for the dipolar contribution of resonant TPA cross-section for intermediate oscillators from the three oscillators model (TOM) for molecule **2** which is similar to three state approximation for

Table 4. Contribution of intermediate oscillators to the most intense TPA peaks.[a]

	1	2	3	4	5	6
1	10.3606	1.4520	3.4440	3.9908	2.4754	0.6715
2	55.9651	9.3333	15.2243	23.4989	14.6803	18.6018
3	8.5616	1.5053	6.4610	20.4621	6.9208	4.6449
4	45.8925	5.9196	22.9896	43.7729	21.8244	16.4075
5	0.2054	0.0113	0.0570	0.1391	0.0230	0.2201
6	2.4634	0.0000	0.0000	0.0000	0.0024	0.0000
7	0.6803	0.0000	0.0000	0.9940	0.0001	0.0005
8	4.3883	0.1864	0.0000	0.4355	5.2090	5.8928
9	0.8854	0.0163	4.6366	0.1520		
10	1.0116	0.2799		3.0123		
11	0.0096	0.0731		0.2930		
12	0.0001	0.0513		1.4280		
13	0.0309	0.0059		0.0014		
14	0.0013	0.0011		0.0004		
15	0.1351	0.0000		0.0002		
16		0.0000		0.0043		
17		0.0091		0.0078		
18		0.0169		0.0049		
TOA	130.6	18.9	52.8	98.3	51.1	46.5
CEO	72.2	45.0	29.3	58.4	27.4	24.1
TOA_rel	2.81	0.41	1.14	2.11	1.10	1
CEO_rel	3.01	1.87	1.22	2.44	1.14	1

[a] Units are in 10^{-34} esu. TOA and CEO represent the values obtained by three oscillators approximation and collective electronic oscillators, respectively. The subscript rel represents the relative values with respect to the values of molecule **6**.

SOS method. TPA1 and TPA2 are the states which absorb two photons, and the lowest four oscillators which are responsible for one-photon absorption are dominant of all the intermediate states in all molecular systems. We thus presented the transition dipole moments only for the lowest four oscillators. The contributions of intermediate oscillators to the most intense TPA peak are given in Table 4 based on TOM. For the calculation TPA, SOS is based on the Eigen states, while CEO is based on oscillators. The most intense TPA peaks are TPA2, TPA3, TPA2, TPA3, TPA2, and TPA2 for molecules **1**, **2**, **3**, **4**, **5**, and **6** and these correspond to the 16th, 19th, 10th, 19th, 9th, and 9th oscillators, respectively. From the TOM, all the intermediate states between the ground and the TPA state can contribute to the TPA cross-sections. In all molecules, the lowest four states are dominant. The first and second states are responsible for the lowest linear absorption (LA1), and the third and fourth ones are for the second lowest linear absorption (LA2). It has often been argued that in many organic molecules the lowest one-photon absorption state is dominant, and the three-state-approximation gives reasonable explanation of linear quadrupolar molecules[17] and a series of symmetrical TPA compounds based on *trans*-stilbene as π center.[14] However, in our systems which have through-space charge transfer interactions, the second linear absorption state(LA2) also plays an important role in the TPA process. In molecules such as **1**, **3**, **4**, **5**, and **6**, the contribution of third linear absorption (LA3) can be significant. The relative TPA cross-section obtained from TOM is in a good agreement with that obtained by CEO except for molecule **2**. This implies that the TPA cross-section of molecule **2** may not be described by simple TOM. In this molecule, two donors and two acceptors are attached at the two upper styryls and two lower styryls of the cyclophane, so there is only through-space and no through-bond charge transfer.

Conclusion

The collective electronic oscillator approach to calculate the frequency-dependent linear and third-order optical response of tetrastyryl-[2,2]paracyclophane derivatives with different combinations of donor and acceptor at the four terminal styryl groups was used. The linear absorption spectra of these through-space charge transfer systems are similar, while the TPA spectra show very different features. All molecules have three main linear absorption peaks and two or three TPA peaks. The TPA states lie 0.3–0.9 eV above the lower-lying two linear absorption states. The investigated molecules have several states which contribute to the TPA cross-section. This is markedly different from other systems such as tetracyanobenzene and diaminobenzene derivatives[17] and stilbene derivatives[14] in which the lowest electronic excited state with strong oscillator strength shows as the most intense peak in linear absorption and consequently dominates the TPA cross-sections. However, as is evident from our study, different combination of functional groups may have very different TPA spectral features even though they may have nearly identical one-photon absorption. One important merit of utilizing through-space intramolecular for TPA applications is that they have many one-photon absorption states which contribute to the TPA cross-section. Through-space couplings could thus be effectively used for fine tuning the molecule for a particular TPA application. The TPA cross-sections obtained by TOM and the CEO give similar trends except for molecule **2** which only has through-space interactions. This issue warrants a further study.

References

1. A. Nag, A. Kr De, D. Goswami, *J. Phys. Conf. Ser.* **2007**, *80*, 012034.
2. A. Colombo, C. Dragonetti, D. Roberto, A. Valore, C. Ferrante, I. Fortunati, A. L. Picone, F. Todescato, J. A. G. Williams, *Dalton Trans.* **2015**, *44*, 15712.
3. B. Sadowski, H. Kita, M. Grzybowski, K. Kamada, D. T. Gryko, *J. Org. Chem.* **2017**, *82*, 7254.
4. D. Kim, H. Moon, S. H. Baik, S. Singha, Y. W. Jun, T. Wang, K. H. Kim, B. S. Park, J. Jung, I. Mook-Jung, K. H. Ahn, *J. Am. Chem. Soc.* **2015**, *137*, 6781.
5. (a) P. Bousso, N. R. Bhakta, R. S. Lewis, E. Robey, *Science* **2002**, *296*, 1876. (b) M. J. Miller, S. H. Wei, I. Parker, M. D. Cahalan, *Science* **2002**, *296*, 1869.
6. P. Feneyrou, O. Doclot, D. Block, P. L. Baldeck, S. Delysse, J. M. Nunzi, *Opt. Lett.* **1997**, *15*, 1132.
7. S. K. Panja, N. Dwivedi, S. Saha, *RSC Adv.* **2016**, *6*, 105786.
8. M. Cha, W. E. Torruellas, G. I. Stegeman, W. H. G. Horsthuis, G. R. Möhlmann, J. Meth, *Appl. Phys. Lett.* **1994**, *65*, 2648.
9. D. Beljonne, J. L. Brédas, M. Cha, W. E. Torruellas, G. I. Stegeman, J. W. Hofstraat, W. H. G. Horsthuis, G. R. Möhlmann, *J. Chem. Phys.* **1995**, *103*, 7834.
10. P. Feneyrou, P. L. Baldeck, *J. Phys. Chem. A* **2000**, *104*, 4764.
11. H. Zhou, X. Zhao, T. Huang, R. Lu, H. Zhang, X. Qi, P. Xue, X. Liu, X. Zhang, *Org. Biomol. Chem.* **2011**, *9*, 1600.
12. S.-J. Chung, K.-S. Kim, T.-C. Lin, G. S. He, J. Swiatkiewicz, P. N. Prasad, *J. Phys. Chem. B* **1999**, *103*, 10741.
13. P. Macak, Y. Luo, P. Norman, H. Ågren, *J. Chem. Phys.* **2000**, *113*, 7055.
14. M. Albota, D. Beljonne, J.-L. Brédas, J. E. Ehrlich, J.-Y. Fu, A. A. Keikal, S. E. Hess, T. Kogej, M. D. Levin, S. R. Marder, D. McCord-Maughon, J. W. Perry, H. Röckel, M. Rumi, G. Subramaniam, W. W. Webb, X.-L. Wu, C. Xu, *Science* **1998**, *281*, 1653.
15. M. Rumi, J. E. Ehrlich, A. A. Heikal, J. W. Perry, S. Barlow, Z. Hu, D. McCord-Maughon, T. C. Parker, H. Röckel, S. Thayumanavan, S. R. Marder, D. Beljonne, J.-L. Brédas, *J. Am. Chem. Soc.* **2000**, *122*, 9500.

16. K. Susumu, J. A. N. Fisher, J. Zheng, D. N. Beratan, A. G. Yodh, M. J. Therien, *J. Phys. Chem. A* **2011**, *115*, 5525.

17. W.-H. Lee, M. Cho, S.-J. Jeon, B. R. Cho, *J. Phys. Chem. A* **2000**, *104*, 11033.

18. B. R. Cho, K. W. Son, S. H. Lee, Y.-S. Song, Y.-K. Lee, S.-J. Jeon, J. H. Choi, H. Lee, M. Cho, *J. Am. Chem. Soc.* **2001**, *123*, 10039.

19. S. K. Pati, T. J. Marks, M. A. Ratner, *J. Am. Chem. Soc.* **2001**, *123*, 7287.

20. M. Drobizhev, A. Karotki, A. Rebane, C. W. Spangler, *Opt. Lett.* **2001**, *26*, 1081.

21. S. J. Lalamam, A. F. Garito, *Phys. Rev. A* **1979**, *20*, 1179.

22. V. J. Docherty, D. Pugh, J. Morley, *J. Chem. Soc. Faraday Trans. 2* **1985**, *81*, 1179.

23. D. R. Kanis, M. A. Ratner, T. J. Marks, M. C. Zerner, *Chem. Mater.* **1991**, *3*, 19.

24. J. F. Ward, *Rev. Mod. Phys.* **1965**, *37*, 1.

25. E. Fadda, M. E. Casida, D. R. Salahub, *Int. J. Quantum Chem.* **2003**, *91*, 67.

26. Y.-Z. Lan, *Comput. Condens. Matter* **2016**, *8*, 22.

27. C. W. Dirk, M. G. Kuzyk, *Phys. Rev. A* **1989**, *39*, 1219.

28. M. G. Kuzyk, C. W. Dirk, *Phys. Rev. A* **1990**, *41*, 5098.

29. J. L. Oudar, *J. Chem. Phys.* **1977**, *67*, 446.

30. M. Blanchard-Desce, M. Barzoukas, *J. Opt. Soc. Am. B* **1998**, *15*, 302.

31. R. Wortmann, P. Kramer, C. Glania, S. Lebus, N. Detzer, *Chem. Phys.* **1993**, *99*, 173.

32. S. R. Marder, D. N. Berattan, L. T. Cheng, *Science* **1991**, *252*, 103.

33. (a) J. Zyss, *J. Chem. Phys.* **1979**, *70*, 3333. (b) J. Zyss, *J. Chem. Phys.* **1979**, *70*, 3341.

34. J. Zyss, *J. Chem. Phys.* **1979**, *71*, 909.

35. L. E. Johnson, L. R. Dalton, B. H. Robinson, *Acc. Chem. Res* **2014**, *47*, 3258.

36. S. Mukamel, S. Tretiak, T. Wagersreiter, V. Chernyak, *Science* **1997**, *277*, 781.

37. S. Mukamel, A. Takahashi, H. X. Wang, G. Chen, *Science* **1994**, *266*, 250.

38. A. Takahashi, S. Mukamel, *J. Chem. Phys.* **1994**, *100*, 2366.

39. S. Mukamel, H. X. Wang, *Phys. Rev. Lett.* **1992**, *69*, 65.

40. S. Tretiak, V. Chernyak, S. Mukamel, *J. Phys. Chem. B* **1998**, *102*, 3310.

41. S. Tretiak, C. Middleton, V. Chernyak, S. Mukamel, *J. Phys. Chem. B* **2000**, *104*, 4519.

42. S. Tretiak, C. Middleton, V. Chernyak, S. Mukamel, *J. Phys. Chem. B* **2000**, *104*, 9540.

43. S. Tretiak, A. Saxena, R. L. Martin, A. R. Bishop, *J. Phys. Chem. B* **2000**, *104*, 7029.

44. T. Toury, J. Zyss, V. Chernyak, S. Mukamel, *J. Phys. Chem. A* **2001**, *105*, 5692.

45. S. Tretiak, S. Mukamel, *Chem. Rev.* **2002**, *102*, 3171 and references therein.

46. G. C. Bazan, W. J. Oldham, R. J. Lachicotte, S. Tretiak, V. Chernyak, S. Mukamel, *J. Am. Chem. Soc.* **1998**, *120*, 9188.

47. J. Zyss, I. Ledoux, S. Volkov, V. Chernyak, S. Mukamel, G. P. Bartholomew, G. C. Bazan, *J. Am. Chem. Soc.* **2000**, *122*, 11956.

48. J. A. Pople, G. A. Segal, *J. Chem. Phys.* **1965**, *43*, S136.

49. J. A. Pople, D. L. Beveridge, P. Dobosh, *J. Chem. Phys.* **1967**, *47*, 2026.

50. J. Ridley, M. C. Zerner, *Theor. Chim. Acta* **1973**, *32*, 111.

51. M. C. Zerner, G. H. Loew, R. F. Kirchner, U. T. Mueller-Westerhoff, *J. Am. Chem. Soc.* **1980**, *102*, 589.

52. J. Ridley, M. C. Zerner, *Theor. Chim. Acta* **1976**, *42*, 223.

53. A. D. Bacon, M. C. Zerner, *Theor. Chim. Acta* **1979**, *53*, 21.

54. J. A. Bjorgaard, M. E. Köse, *RSC Adv.* **2015**, *5*, 8432.

55. M. J. S. Dewar, E. G. Zoebisch, E. F. Healy, J. J. P. Stewart, *J. Am. Chem. Soc.* **1985**, *107*, 3902.

56. P. A. Dirac, *Proc. Camb. Philol. Soc.* **1930**, *26*, 376.

57. S. Tretiak, V. Chernyak, S. Mukamel, *J. Am. Chem. Soc.* **1997**, *119*, 11408.

58. S. Tretiak, V. Chernyak, S. Mukamel, *Chem. Phys. Lett.* **1996**, *259*, 55.

59. (a) Y. Saad, *Numerical Methods for Large Eigenvalue Problems*, University Press, Manchester, **1992**. (b) V. Chernyak, M. F. Schultz, S. Mukamel, S. Tretiak, E. V. Tsiper, *J. Chem. Phys.* **2000**, *113*, 36.

60. (a) E. R. Davidson, *J. Comput. Phys.* **1975**, *17*, 87. (b) E. R. Stratmann, G. E. Scuseria, M. J. Frisch, *J. Chem. Phys.* **1998**, *109*, 8218.

61. K. B. Wiberg, E. R. Stratmann, M. Frisch, *J. Chem. Phys. Lett.* **1998**, *297*, 60.

62. J. Y. Lee, *Bull. Kor. Chem. Soc.* **2003**, *24*, 780.

63. E. J. Cho, J. W. Moon, S. W. Ko, J. Y. Lee, S. K. Kim, J. Yoon, K. C. Nam, *J. Am. Chem. Soc.* **2003**, *125*, 12376.

64. J. Y. Lee, E. J. Cho, S. Mukamel, K. C. Nam, *J. Org. Chem.* **2004**, *69*, 943.

65. B. S. Hudson, B. E. Kohler, *Annu. Rev. Phys. Chem.* **1974**, *25*, 437.

66. B. S. Hudson, B. E. Kohler, K. Schulten, In *Excited States*, Vol. *6*, E. C. Lim Ed., Academic Press, New York, **1982**, p. 1.

67. S. Tretiak, V. Chernyak, S. Mukamel, *Int. J. Quantum Chem.* **1998**, *70*, 711.